International Journal of Impact Engineering 109 (2017) 67–77

Contents lists available at ScienceDirect

International Journal of Impact Engineering

journal homepage: www.elsevier.com/locate/ijimpeng

Stability of tungsten projectiles penetrating adobe masonry – Combined experimental and numerical analysis

C. Sauer, A. Heine*, K.E. Weber, W. Riedel

Fraunhofer EMI, Eckerstr. 4, 79104 Freiburg, Germany

ARTICLE INFO

Article History:
Received 12 April 2017
Revised 2 June 2017
Accepted 4 June 2017
Available online xxx

Keywords:
Adobe masonry
WHA projectiles
Hydrocode simulation
Impact
RHT model

ABSTRACT

We investigate the penetration of tungsten-heavy-alloy projectiles into adobe targets. The analysis rests on two complementary parts. Firstly, experimental data comprising impact experiments with five different projectile variants against finite-thickness adobe targets is available. Although the data stems from earlier work, it is presented in full detail here for the first time. The general phenomenology is discussed mainly with respect to projectile failure and stability of the penetration in adobe. Secondly, a recently published hydrocode model for adobe under impact loading is applied without further modification for complementing the experimental results with additional time-resolved insight into the penetration mechanics. For the regime without projectile failure or significant plastic deformation, this hydrocode model is capable of reproducing the experimentally observed projectile-target interaction with good overall agreement between experiments and simulation. While the test data covers different penetration regimes from rigid-body motion to projectile failure, the numerical analysis is restricted to linear-elastic behavior of the impactors, in order to avoid any ambiguity due to the less established projectile material description. With the information from the hydrocode simulations, we are able to reveal the origin of the projectile-specific magnitude of instability in the penetration in adobe. The thereby achieved understanding of the motion of the differently shaped impactors within the formed cavity allows us to discuss possible explanations for the particular projectile failure observed in the experimental data.

1. Introduction

In the present paper, we study the interaction of high-strength projectiles with a low-strength building material. The considered projectiles are homogeneous tungsten-heavy-alloy (WHA) penetrators of different shapes. Fascinatingly, the interaction of such projectiles tends to become more complex for decreasing density and strength of the target material. For example, the penetration of WHA penetrators into semi-infinite steel typically goes along with a monotonic increase of the penetration depths and a transition from rigid-body behavior to erosion when the impact velocity gets larger [1–3]. Furthermore, the penetration craters tend to be straight. For aluminum, instabilities occur for intermediate velocities [4]. In this regime, the penetration craters bend and the projectiles show fracturing. Only at higher velocities straight craters, accompanied by penetrator erosion, as well as a monotonic increase of penetration with impact velocity are resumed. Similar types of behavior are observed for concrete [5]. For the adobe masonry brick material discussed in the present paper, the phenomena are even more complex. For steel spheres penetrating into adobe, the depth-of-penetration shows a maximum at finite velocity [6], clearly differing from the behavior known for metals and in certain aspects similar to observations made for sand [7] or graphite [8]. For WHA projectiles, penetration stability and projectile failure are strongly dependent on impact velocity and projectile shape when impacting adobe targets [9,10].

Thus, although at first sight counterintuitive, the interaction of WHA projectiles becomes more complex for weaker targets. Such a situation demands for a deeper analysis and it is obvious to pursue an integrated approach of testing and modeling. The numerical simulations presented in this paper are based on a recently published constitutive model for adobe [11], applied in finite-element-methods of the hydrocode type. They solve partial differential equations derived from the conservation of mass, momentum and energy using explicit time integration schemes. The following study shows how these simulations lead to a deeper scientific understanding of the underlying mechanical processes that trigger the different penetration phenomena in adobe.

In Section 2, the paper starts with a detailed description of the available experimental data and the key phenomenological findings. Afterwards, a comparison of results from exemplary hydrocode simulations with the corresponding data from the experiments is presented in the first part of Section 3. The agreement between the results from the simulations and the experiments with elastic

* Corresponding author.
E-mail address: andreas.heine@emi.fraunhofer.de (A. Heine).

http://dx.doi.org/10.1016/j.ijimpeng.2017.06.001
0734-743X/

projectile behavior enables us to reveal the origin of the observed projectile-specific penetration behavior through further investigation of the simulations. Additionally, possible reasons for the particular failure of the projectiles are discussed. Finally, overall scientific conclusions from the integrated experimental and numerical analysis are given in Section 4.

2. Review of experiments

The baseline for the analyses of the present paper are results from test series that were in part shown and discussed before in several communications [9,10,12]. However, a presentation in full detail is so far lacking in literature. Therefore, this section includes a coherent summary of all own tests including tabulated values for impact velocities, yaw angles, residual lengths, and residual velocities of the projectiles. In addition, flash X-rays for a large fraction of the experiments are shown. This extended presentation allows to further elaborate the key phenomena in different penetration regimes. All this provides a database for the combined experimental and numerical analysis of the present paper as well as a potential starting point for further investigations.

2.1. Experimental parameters

In total five different types of projectiles were considered, see Fig. 1. They differ regarding nose shape, mass, length, and diameter. The material used for the projectiles is WHA. A full overview of dimensions and material properties is provided in Table 1.

The projectiles were accelerated with a laboratory gun to velocities in the range from approximately 300 m/s to 2000 m/s, see below for details. The considered targets were composed of adobe bricks with nominal dimensions 240 mm × 115 mm × 71 mm, a density of 1.8 g/cm^3, and a compressive strength of 3–5 N/mm^2. Although these bricks originate from two different lots, they are well characterized by the given values and can be considered equal for the applications in this work.

In order to achieve a substantial distance between impact location and lateral boundary, the bricks were oriented upright. In most of the tests, four bricks were placed in series resulting in a nominal target thickness of 284 mm. Additional bricks at the sides and a steel frame were used to achieve a certain level of confinement, similar to the conditions in a masonry wall section. This configuration is shown schematically in Fig. 2, upper part. Some tests with projectile type 3 at low impact velocities were done with a slightly different target configuration, where a single row of bricks was used and loaded vertically with steel plates (Fig. 2, lower part). In this setup, the target thickness was varied from 71 mm to 497 mm. The vertical load was adjusted to approximately 3.6 kPa in all tests done with this setup (a loading mass of around 3 kg per nominal brick cross section of 71 mm × 115 mm).

Table 1
Properties of the projectiles illustrated in Fig. 1. Material parameters stem from [13].

Projectile type	1	2	3	4	5
Nose shape	Ogival	Truncated	Truncated	Ogival	Ogival
Overall length L [mm]	30	45	90	55	90
Maximum diameter D [mm]	8	6	6	8	6
Length of cylindrical part [mm]	19.4	36.0	81.0	44.4	80.7
Nose radius [mm]/Cone angle [°]	16.0/–	–/15.0	–/15.0	16.0/–	16.0/–
L/D	3.8	7.5	15.0	6.9	15.0
Mass m [g]	23	23	46	46	46
Density [g/cm^3]			17.6		
Yield strength $R_{p0.2}$ [N/mm^2]			1290		
Ultimate tensile strength [N/mm^2]			1380		
Elongation at fracture A_5 [%]			11		

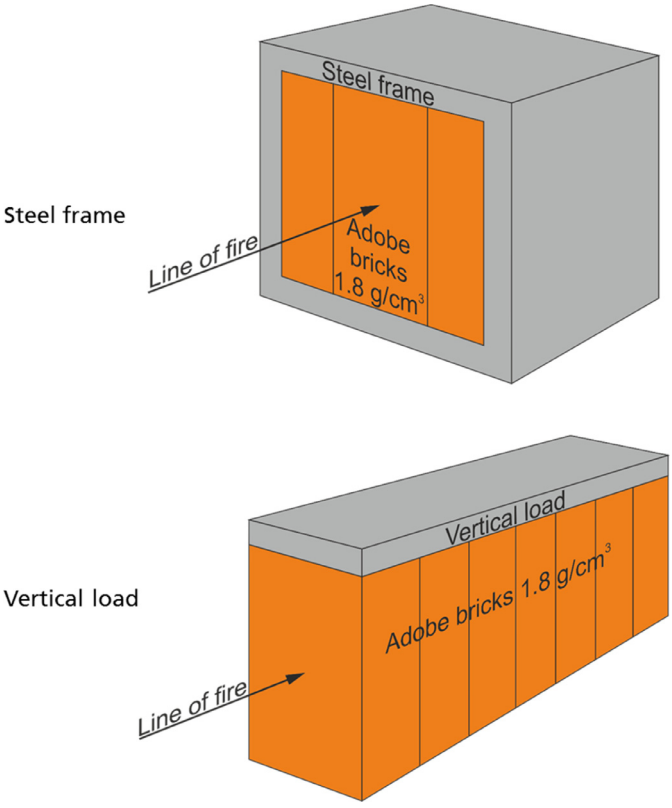

Fig. 2. Schematic configurations of the targets utilized in the experiments summarized in Table 2.

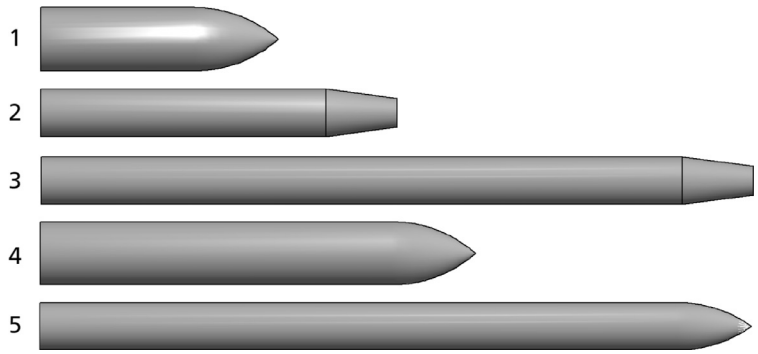

Fig. 1. Geometry of projectile variants 1–5, varying from ogive to truncated nose shapes and in L/D ratio.